

# Tsunami and tephra deposits record interactions between past eruptive activity and landslides at Stromboli Volcano

**Marco Pistolesi<sup>1</sup>, Antonella Bertagnini<sup>2</sup>, Alessio Di Roberto<sup>2</sup>, Maurizio Ripepe<sup>3</sup> and Mauro Rosi<sup>1</sup>**

*<sup>1</sup>Dipartimento di Scienze della Terra, Università di Pisa, via S. Maria 53 - 56126 Pisa (Italy)*

*<sup>2</sup>Istituto Nazionale di Geofisica e Vulcanologia, via della Faggiola 32 - 56126 Pisa (Italy)*

*<sup>3</sup>Dipartimento di Scienze della Terra, Università di Firenze, via G. La Pira 4 - 50121 Firenze (Italy)*

## **METHODS**

Three trenches were dug with the use of a mechanical excavator in the north-eastern sector of Stromboli volcano (Italy), from ~170 m to ~260 m from the current coast line (Figs. 1, 2). As already observed during the 2002 event, this area represents a low-energy coastal zone, where the tsunami waves generated on the northern side of the island, are partially attenuated by the seafloor. Despite the wave attenuation, the flat subaerial topography represents a zone easily invaded and a high-preservation potential area for the deposits left by the tsunami wave. Along the shoreline, the coast is characterized by a ~100 m-wide beach of black sand with rounded cobbles and pebbles of lavas.

The combination of a wide beach made of loose materials with different size (from sand to cobbles), represents an ideal setting for charging the penetrating wave with heterometric sediment. Conversely, the presence of a wide, gently inclined, flat back-dune area where the wave can freely spread and gradually lose its energy and carrying capacity, represents a favorable setting for the

formation of thick deposits preserved thanks to the rapid burial under ash and tephra produced by the continuous activity of the volcano.

Trench 1 is the most distal from the coastline (from 215 to 245 m from the shore) and is located at 3.5 to 4.2 m of above sea level (a.s.l.). It consists of a main branch oriented parallel to the coast line (30 m-long) and two branches (left 26 m- and right 10 m-long) perpendicular to the main section and to the coast line. Trenches 2 and 3 are located at an elevation of 3.5 and 3.8 m a.s.l., respectively; these are approximately 8 and 4 m in length, respectively and are both oriented parallel to the coastline. Accurate values of the trenches corners and of the absolute heights above sea levels of the sandy and tephra layers were obtained by means of GPS and total station theodolite. Topographic profiles were obtained through GIS data analysis by using a grid raster base  $1 \times 1$  m-spaced with vertical accuracy of 20 cm. These were further constrained with topographic control points from the total station (Fig. 2).

From each trench, samples from the loose sandy, cobbles-bearing deposits, from the interlayered tephra layers, soils and charcoals were recovered (Fig. DR1). Analysis of the grain-size distribution of sand-rich deposits and tephra layers were carried out in the laboratory by means of mechanical dry sieving. Samples were sieved at one  $\phi$  ( $\phi = -\log_2$  of the grain diameter) intervals for the  $-5 \phi$  (16 mm) to  $+5 \phi$  (0.032 mm) size range. Diameter of clast larger than  $-5 \phi$  (16 mm) were measured using a  $1 \phi$ -sized metal template. The median ( $Md_\phi$ ), sorting ( $\sigma_\phi$ ), skewness ( $S_{K1}$ ) and kurtosis ( $K_G$ ) were calculated from the grainsize distribution and the deposits are classified according to Folk (1954) and are reported in Table DR1.

Size analysis of the pebble, cobble and boulder fraction was carried out in the field at variable distance from the shoreline by measuring with a caliper the maximum (a), intermediate (b) and minimum (c) axes of all single particles to calculate Elongation ( $b/a$ ) and Flatness ( $c/b$ ) parameters. The morphological analysis of particles  $>-1\phi$  (2 mm) was also performed. High-resolution 2D digital images (24 megapixels) were acquired with a digital camera, and shape parameters were calculated on the binarized projected outline of each particle using the ImageJ freeware software

(Schneider et al., 2012). The form factor (which compares the surface of the object to the surface of the disc with same perimeter) and convexity (perimeter/perimeter of the convex bounding polygon) parameters were calculated for each particle (Liu et al., 2015).

Textural characteristics of the particles were analyzed with a Zeiss EVO 304 MA 10 scanning electron microscope (SEM) at Istituto Nazionale di Geofisica e Vulcanologia (Pisa). Major elements glass compositions of tephra were carried out using an ISIS-Oxford micro-analytical system linked to the SEM. Data were collected at an acceleration voltage of 15 Kev, using a 300pA current probe and an acquisition time of 100 s. Concentrations were obtained after ZAF correction using natural minerals or pure oxides for calibration.

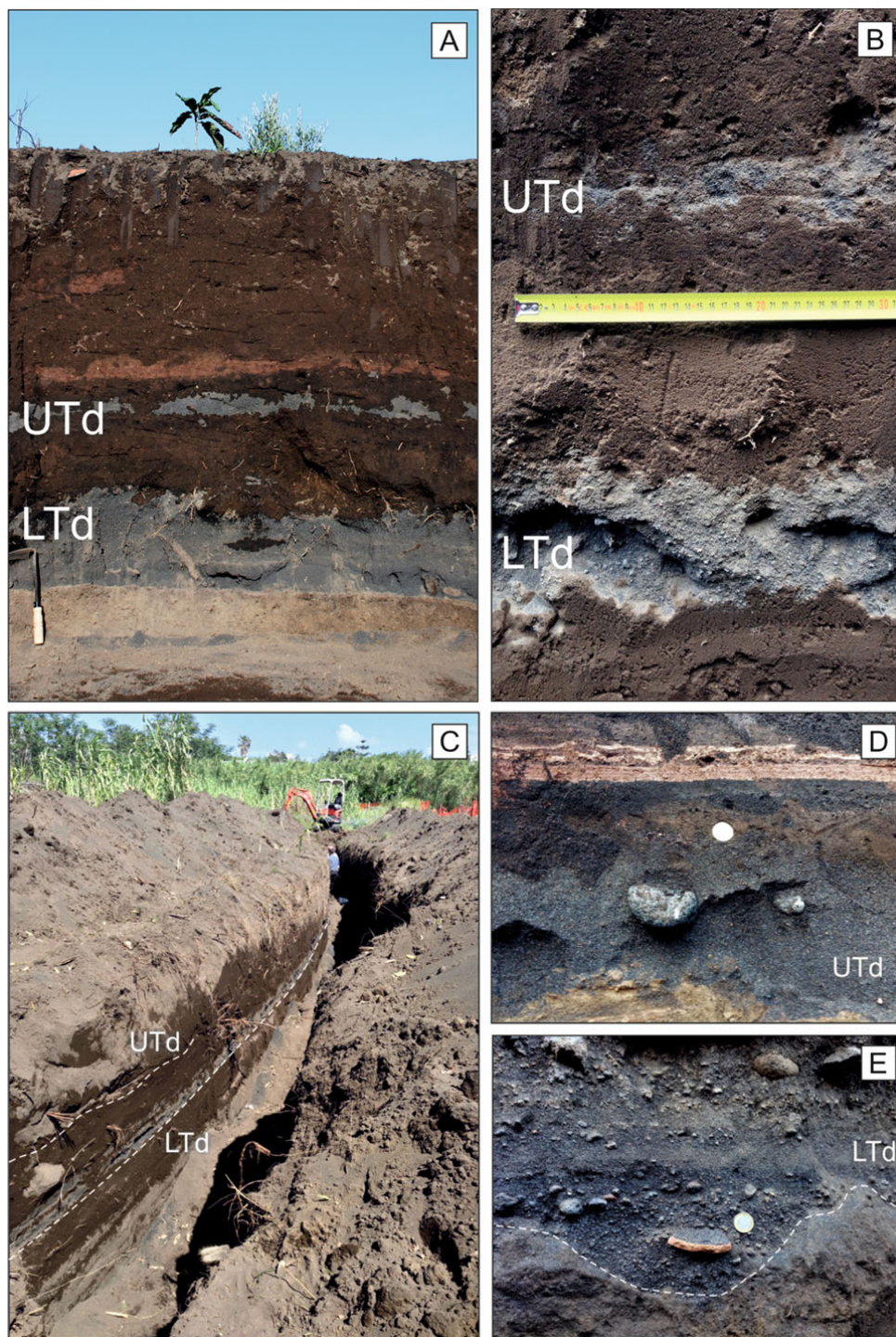


**Figure DR1.** (A) Photo of the tephra and tsunami sequence in Trench 2 (tool for scale is 20 cm). (B) A detail of LTd and UTd in Trench 1. (C) Picture showing one of the branch of Trench 1, where the lateral continuity of the sandy beds is highlighted by the white dashed lines. (D) and (E) show details of the tsunami deposits in Trenches 2 and 3, respectively.

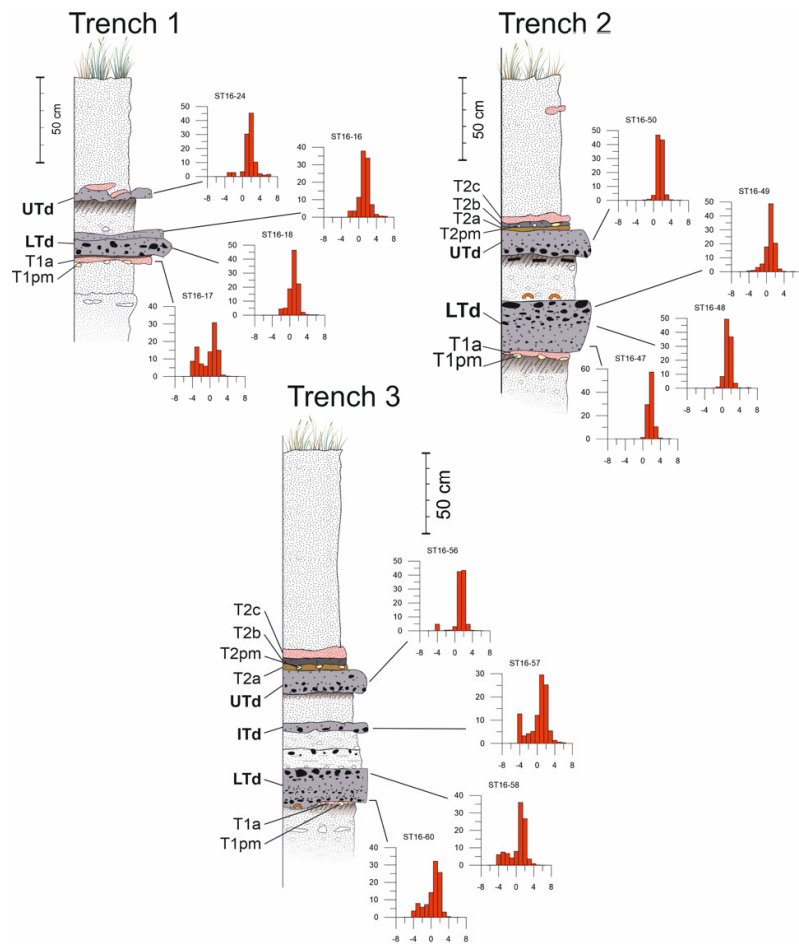


**Figure DR2.** Grain-size histograms of representative matrix sand deposits collected in the three trenches.

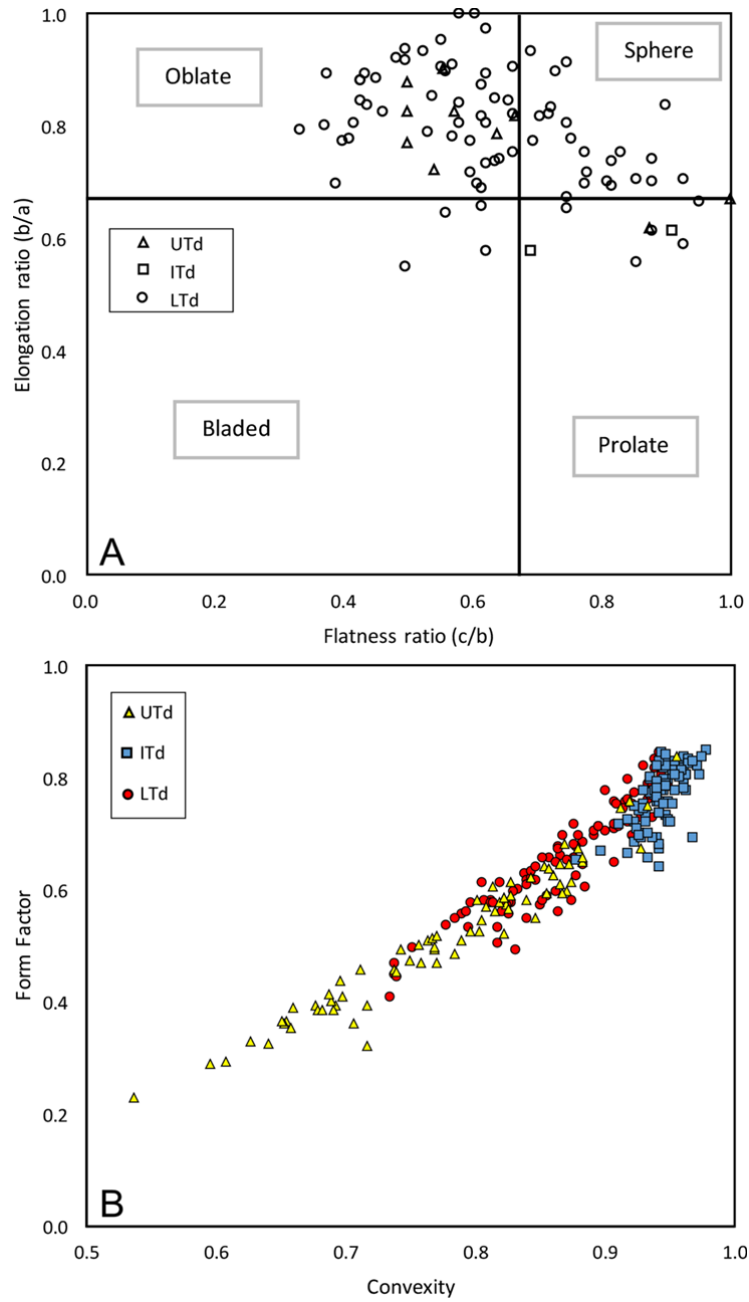


**Figure DR3.** (A) Elongation ( $b/a$ ) vs flatness ( $c/b$ ) ratio obtained from the measurement of the three axes of ~100 pebbles randomly collected from each deposit at various outcrops. (B) Form factor vs convexity measured on ~265 smaller clasts (size range 2-16 mm) from the three tsunami deposits.



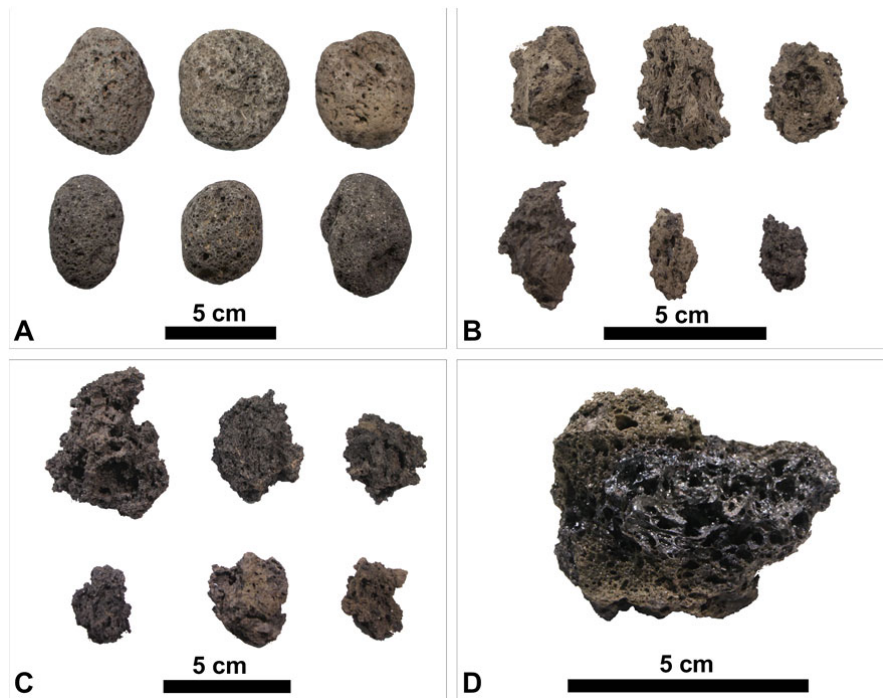


**Figure DR4.** (A) Exemples of pebbles collected in LTd. (B) Pumice clasts from the T2 pumice layer. (C) Scoriaceous and mingled clasts from the T2 pumice layer. (D) Detail of a pumiceous clast from T2 pumice layer.

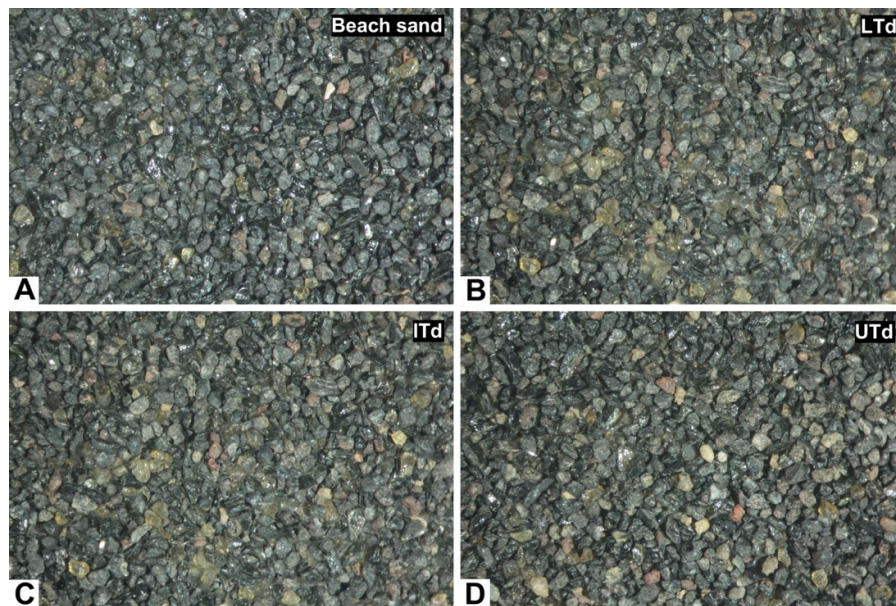


**Figure DR5.** Comparison among the <2 mm size fractions from the present beach sand (A), LTd (B), ITd (C) and UTd (D).

**Table DR1.** Labels, locations and sedimentological parameters of the samples analyzed in this work.

| Sample  | UTM                | Trench | Str.<br>height | Md $\phi$ | $\sigma\phi$ | Sediment classification                 | S <sub>KI</sub> | K <sub>G</sub> | Gravel<br>(%) | Sand<br>(%) | Silt<br>(%) |
|---------|--------------------|--------|----------------|-----------|--------------|---|-----------------|----------------|---------------|-------------|-------------|
| ST16-33 | 33S 520890 4294929 | beach  | -              | 1.28      | 0.71         | Slightly Very Fine Gravelly Medium Sand | 1.49            | 1.00           | 0.17          | 99.26       | 0.57        |
| ST16-16 | 33S 520890 4294929 | 1      | LTd            | 0.84      | 1.01         | Fine Gravelly Coarse Sand               | 0.77            | 1.27           | 6.98          | 91.82       | 1.20        |
| ST16-17 | 33S 520890 4294929 | 1      | LTd            | -0.21     | 2.29         | Sandy Medium Gravel                     | -1.02           | 0.67           | 38.77         | 61.09       | 0.14        |
| ST16-18 | 33S 520890 4294929 | 1      | LTd            | 0.47      | 1.04         | Very Fine Gravelly Coarse Sand          | 0.29            | 1.31           | 9.50          | 89.99       | 0.51        |
| ST16-22 | 33S 520890 4294929 | 1      | LTd            | 0.42      | 1.19         | Coarse Gravelly Coarse Sand             | 0.01            | 1.72           | 15.61         | 84.18       | 0.21        |
| ST16-23 | 33S 520890 4294929 | 1      | LTd            | 0.62      | 0.99         | Very Fine Gravelly Coarse Sand          | 0.63            | 1.22           | 6.46          | 92.50       | 1.03        |
| ST16-24 | 33S 520890 4294929 | 1      | UTd            | 1.23      | 0.88         | Medium Gravelly Medium Sand             | 1.11            | 1.70           | 5.71          | 91.65       | 2.65        |
| ST16-37 | 33S 520890 4294929 | 1      | LTd            | 0.32      | 1.67         | Medium Gravelly Coarse Sand             | -0.48           | 1.26           | 22.10         | 77.10       | 0.80        |
| ST16-38 | 33S 520890 4294929 | 1      | LTd            | 0.38      | 1.78         | Fine Gravelly Coarse Sand               | -0.58           | 1.31           | 21.83         | 77.46       | 0.71        |
| ST16-39 | 33S 520890 4294929 | 1      | LTd            | 1.00      | 0.83         | Slightly Very Fine Gravelly Medium Sand | 1.18            | 1.06           | 1.94          | 97.0        | 1.06        |
| ST16-47 | 33S 520913 4294928 | 2      | LTd            | 1.33      | 0.72         | Slightly Very Fine Gravelly Medium Sand | 1.52            | 1.07           | 0.11          | 99.47       | 0.43        |
| ST16-48 | 33S 520913 4294928 | 2      | LTd            | 0.82      | 0.78         | Slightly Very Fine Gravelly Coarse Sand | 1.29            | 0.91           | 0.91          | 98.49       | 0.59        |
| ST16-49 | 33S 520913 4294928 | 2      | LTd            | 0.45      | 1.01         | Very Fine Gravelly Coarse Sand          | 0.21            | 1.38           | 10.37         | 89.43       | 0.26        |
| ST16-50 | 33S 520913 4294928 | 2      | UTd            | 0.96      | 0.75         | Slightly Very Fine Gravelly Coarse Sand | 1.35            | 0.74           | 1.26          | 98.35       | 0.39        |
| ST16-56 | 33S 520933 4294905 | 3      | UTd            | 0.97      | 0.79         | Very coarse Gravelly Coarse Sand        | 1.20            | 1.60           | 5.85          | 93.98       | 0.17        |
| ST16-57 | 33S 520933 4294905 | 3      | ITd            | 0.42      | 2.34         | Coarse Gravelly Coarse Sand             | -0.75           | 1.22           | 25.42         | 73.64       | 0.94        |
| ST16-58 | 33S 520933 4294905 | 3      | LTd            | 0.48      | 2.12         | Medium Gravelly Coarse Sand             | -0.74           | 1.15           | 24.65         | 75.19       | 0.16        |
| ST16-59 | 33S 520933 4294905 | 3      | LTd            | 1.13      | 0.92         | Fine Gravelly Medium Gravel             | 0.91            | 1.57           | 10.77         | 88.80       | 0.44        |
| ST16-60 | 33S 520933 4294905 | 3      | LTd            | 0.35      | 1.87         | Medium Gravelly Coarse Sand             | -0.57           | 1.11           | 24.60         | 75.37       | 0.03        |
| ST16-15 | 33S 520890 4294929 | 1      | T1a            | 2.73      | 1.93         | Fine ash                                | 1.13            | 0.90           |               |             |             |
| ST16-25 | 33S 520890 4294929 | 1      | T2c            | 3.06      | 1.48         | Very fine ash                           | 1.85            | 0.87           |               |             |             |
| ST16-61 | 33S 520933 4294905 | 3      | T1a            | 3.23      | 1.64         | Very fine ash                           | 1.52            | 0.97           |               |             |             |
| ST16-55 | 33S 520933 4294905 | 3      | T2a            | 2.59      | 1.29         | Fine ash                                | 2.05            | 1.00           |               |             |             |
| ST16-53 | 33S 520933 4294905 | 3      | T2b            | 2.11      | 1.15         | Fine ash                                | 2.10            | 1.07           |               |             |             |
| ST16-52 | 33S 520933 4294905 | 3      | T2c            | 2.03      | 1.40         | Fine ash                                | 1.32            | 0.88           |               |             |             |



### **Additional references**

- Folk, R.L., 1954, The distinction between grainsize and mineral composition in sedimentary-rock nomenclature: *J. Geology*, 62, 344-359.
- Liu, E.J., Cashman, K.V., and Rust, A.C., 2015, Optimising shape analysis to quantify volcanic ash morphology: *GeoResJ*, 8, 4–30, doi: 10.1016/j.grj.2015.09.001.
- Schneider, C.A., Rasband, W.S., Eliceiri, K.W., 2012, NIH Image to ImageJ: 25 years of image analysis: *Nature Methods*, 9, 671, <https://doi.org/10.1038/nmeth.2089>.